Supplement of

Contribution of free tropospheric aerosols to Arctic low-level cloud droplets and longwave emissivity

Roman Pohorsky, Heather Guy, Ian M. Brooks, Lea Haberstock, Nicolas Fauré, Paul Zieger, Julia Kojoj, Sonja Murto, Radiance Calmer, Benjamin Heutte, Michael Lonardi, Erik S. Thomson, Michael Tjernström, Jessie Creamean, Athanasios Nenes, Julia Schmale

Correspondence to: Roman Pohorsky (roman.pohorsky@epfl.ch) and Julia Schmale (julia.schmale@epfl.ch)

Supplemental information

Table S1 List of Helikite flights during the ARTofMELT campaign. Indicated take-off and landing times are in UTC. A cloud value of 0 indicates either a clear sky day or a cloud base higher than the maximum reached altitude of the Helikite during the flight. A value of 1 indicates that the Helikite sampled in a cloud but did not reach above cloud top. A value of 2 indicates that the Helikite went above the cloud top. The deployment of each instrument is listed in different columns, with 1 meaning the instrument was present and 0 not present. ST stands for SmartTether.

Flight	Date	Take off	Landing	Max altitude (m)	Cloud	ST	POPS	mSEMS	LOAC
1	2023-05-16	20:01:02	20:42:49	267	0	1	1	1	1
2	2023-05-17	11:23:33	13:45:48	441	0	1	1	1	1
3	2023-05-18	09:54:52	13:40:22	503	2	1	1	1	0
4	2023-05-18	14:47:00	19:02:06	482	0	1	1	1	0
5	2023-05-19	14:27:22	17:57:00	479	0	1	1	1	0
6	2023-05-23	11:51:05	14:24:48	368	1	1	1	1	0
7	2023-05-23	14:56:57	17:36:30	556	2	1	1	1	0
8	2023-05-29	10:46:24	12:10:36	246	0	0	1	1	1
9	2023-05-29	14:01:30	16:34:23	454	0	1	1	1	1
10	2023-06-02	10:09:48	12:12:31	443	0	1	1	1	1
11	2023-06-02	14:30:26	20:03:38	496	1	1	1	0	1
12	2023-06-03	14:24:57	14:45:26	205	1	1	1	1	0
13	2023-06-03	14:53:10	17:16:45	657	2	1	1	1	0
14	2023-06-04	13:47:38	16:27:19	560	2	1	1	1	0
15	2023-06-04	17:02:38	21:02:16	403	2	1	1	1	0
16	2023-06-06	14:14:00	20:26:32	547	0	1	1	0	1
17	2023-06-07	10:10:03	13:52:26	410	2	1	1	1	0
18	2023-06-07	14:31:06	17:35:44	481	2	1	1	1	0
19	2023-06-07	19:09:04	22:13:54	580	2	1	1	1	0
20	2023-06-09	09:31:50	11:39:02	533	0	1	1	1	0
21	2023-06-10	10:06:46	12:57:46	474	1	1	1	1	1
22	2023-06-10	13:41:48	16:50:50	466	2	1	1	1	1
23	2023-06-10	17:19:25	20:05:40	468	1	1	1	1	1

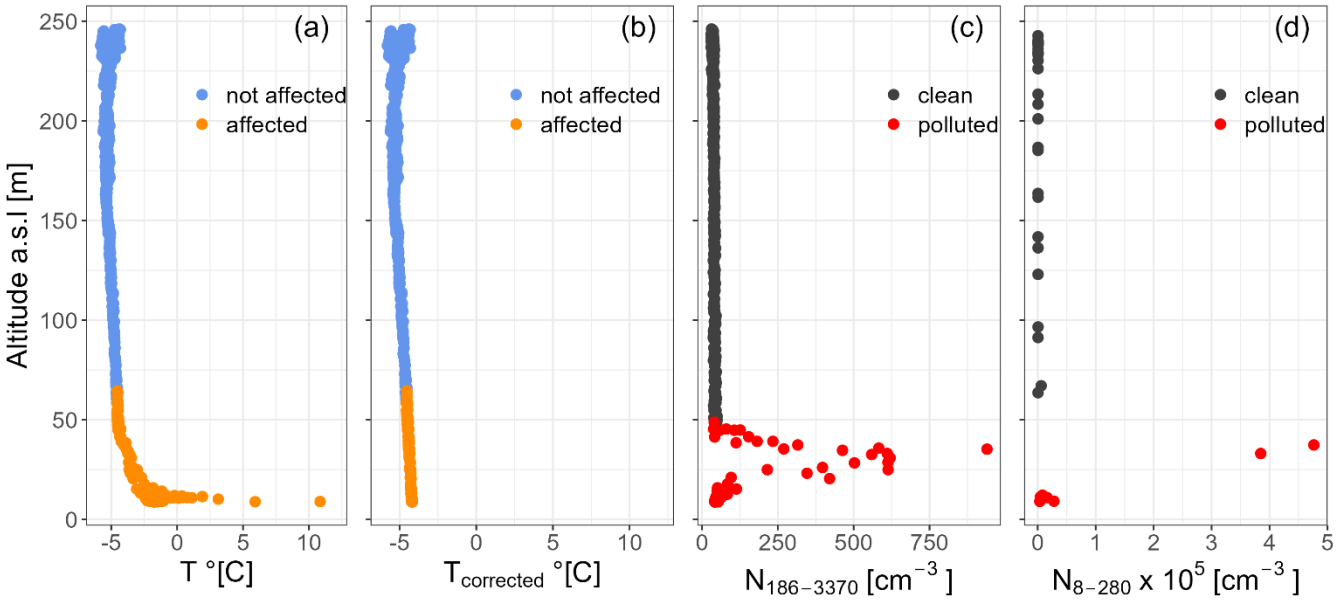

Figure S1 Example profiles from flight 8 on May 29, 2025 of (a) temperature, (b) corrected temperature, (c) $N_{186-3370}$ and (d) $N_{186-3370}$. For temperature profiles, the color indicates temperature measurements affected by the ship's heat, which is corrected in (b). For aerosol profiles, the red dots correspond to the identified ship pollution.

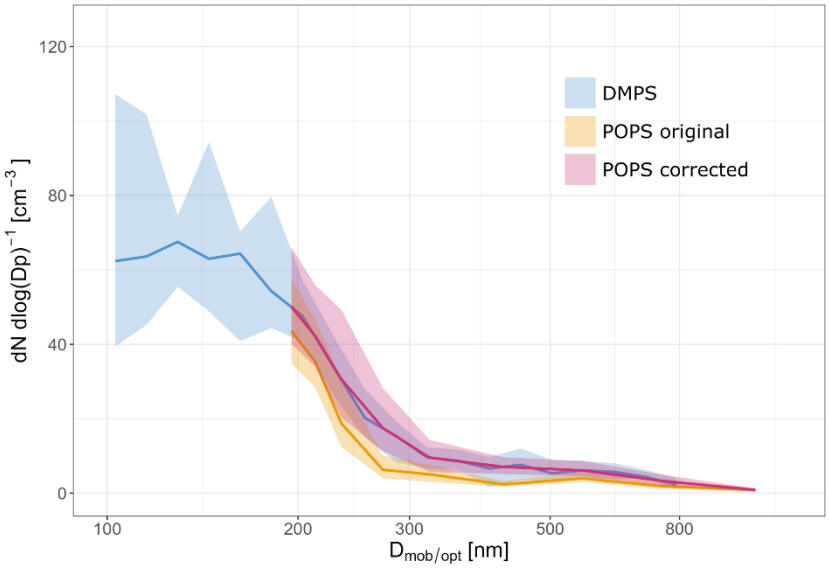

Figure S2 Size distribution measured with the DMPS and POPS during the ship-based intercomparison. The pink size distribution represents the corrected concentrations after the correction factors have been applied.

Table S2 Correction factors applied to the POPS original concentration values per bin.

POPS bin	Midpoint diameter (nm)	Multiplication factor
b3	195	1.15
b4	212	1.19
b5	234	1.63
b6	272	2.78
b7	322	1.89
b8	422	2.98
b9	561	1.53
b10	748	1.77
b11	1054	1
b12	1358	1
b13	1802	1
b14	2440	1
b15	3061	1

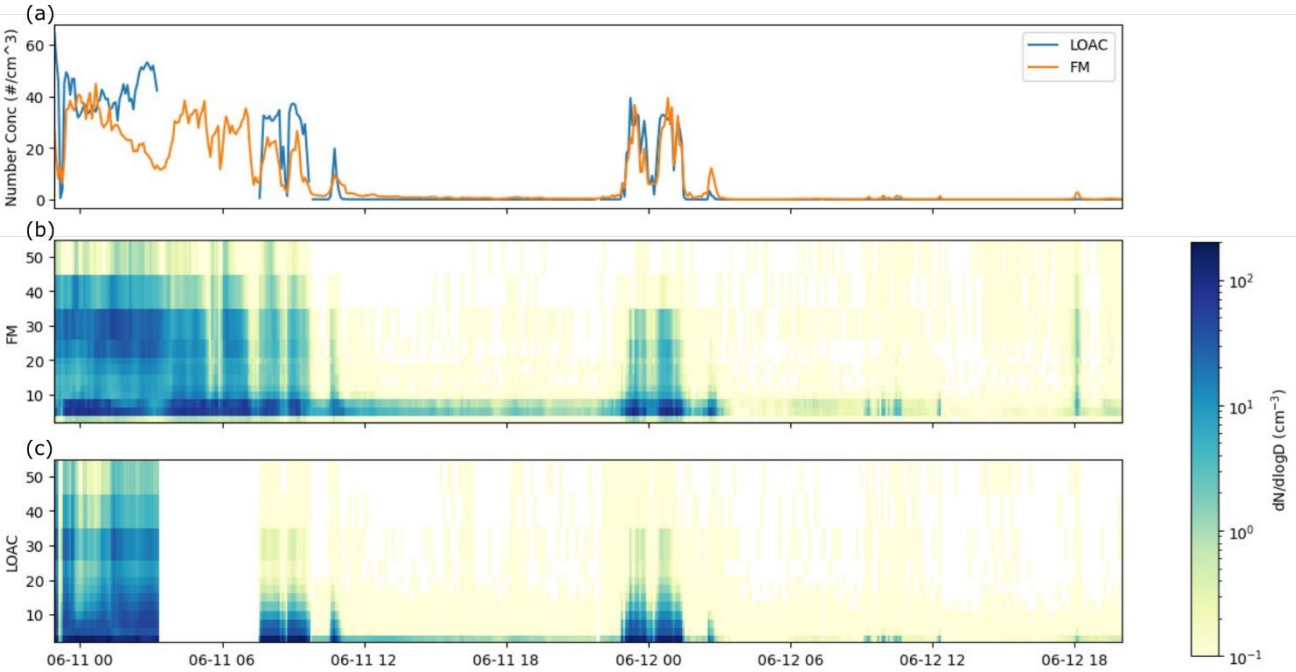

Figure S3 Intercomparison of the LOAC and Fog monitor between June 10 and June 11, 2023 on top of the aerosol-cloud laboratory on the fourth deck. (a) Total droplet number concentration measured by each instrument. (b) Heatmap of the cloud droplet size distribution measured by the Fog Monitor. (c) Heatmap of the cloud droplet size distribution measured by the LOAC.

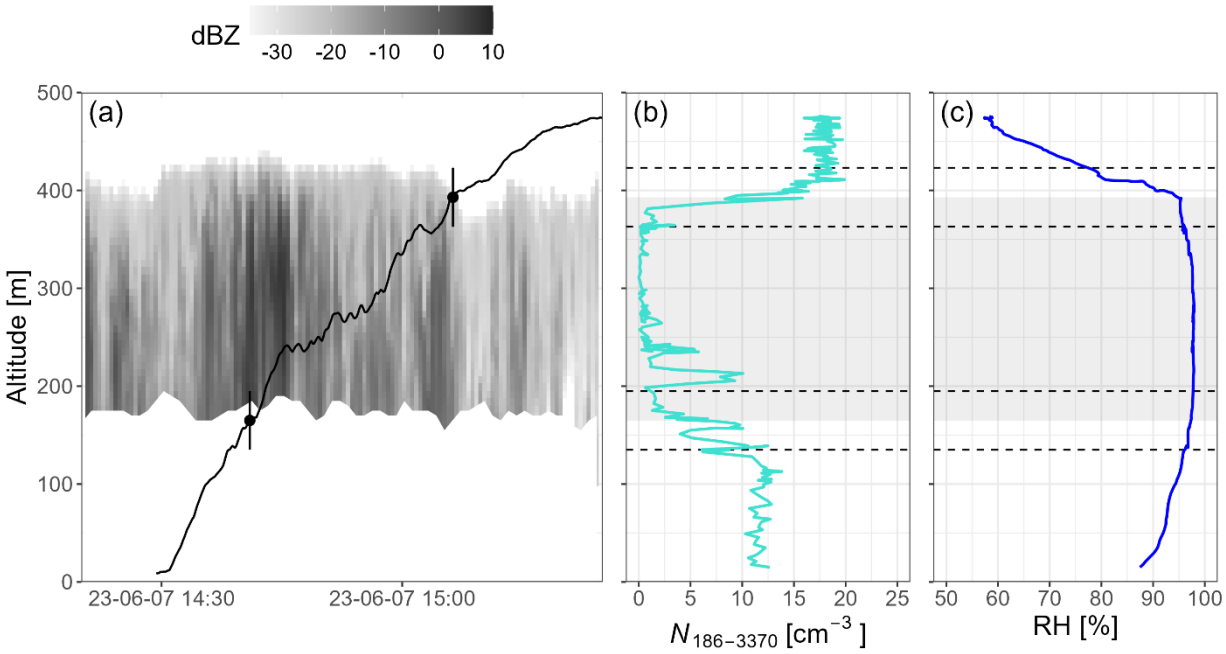

Figure S4 Example of cloud boundaries identification. On panel (a), grey filling indicates the cloud radar reflectivity and the trace represents the Helikite altitude. Panels (b) and (c) show vertical profiles of particle number concentration between 186 and 330 nm and RH, respectively. The cloud boundaries represented by dots in (a) and grey shading in (b) and (c) were identified at 393 m a.m.s.l for the top and 165 m for the base. A ± 30 m uncertainty on the cloud boundaries is indicated by vertical error bars in (a) and horizontal dashed line in (b) and (c).

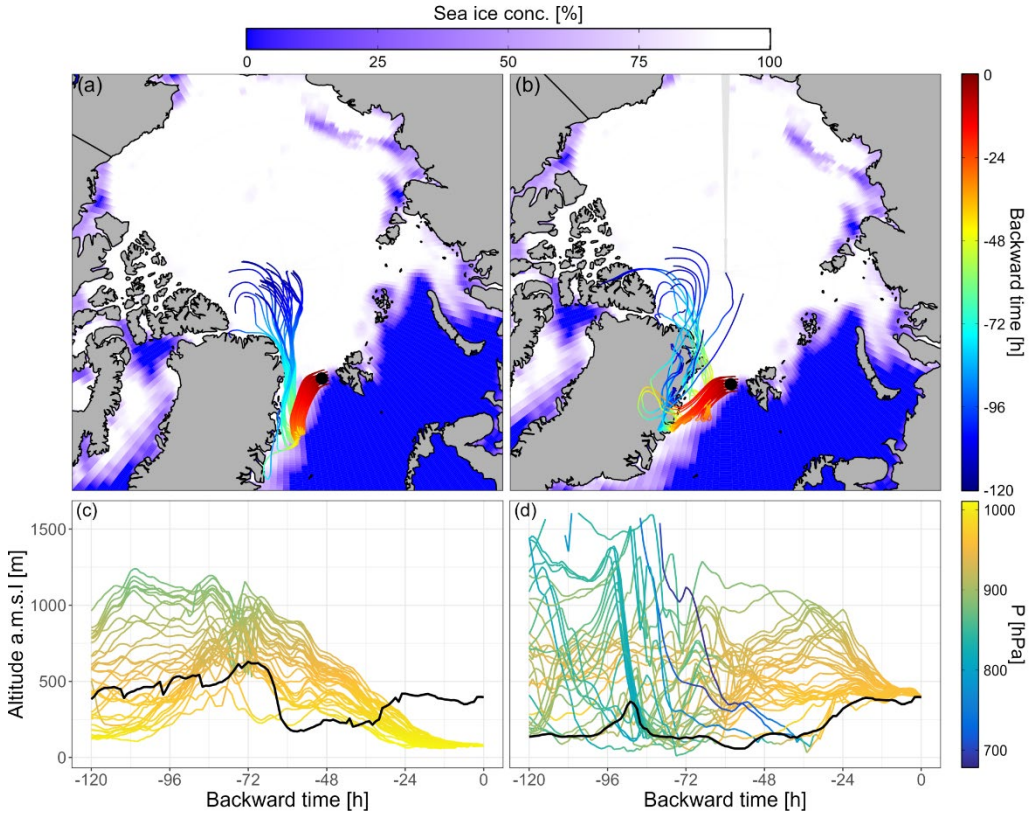

Figure S5 Five-day backtrajectory analysis of air masses arriving at the ship location on June 7th at 12:00 UTC. The 37 backtrajectories were calculated with the LAGRANTO model. (a) and (c) Trajectories arriving at the surface (1013 hPa). Panels (b) and (d) Trajectories arriving above the boundary layer (950 hPa). The top panels show the horizontal path of the air masses and the bottom panels show the vertical path. On the bottom panels, the average depth of the atmospheric boundary layer along the air mass path is shown (black line).

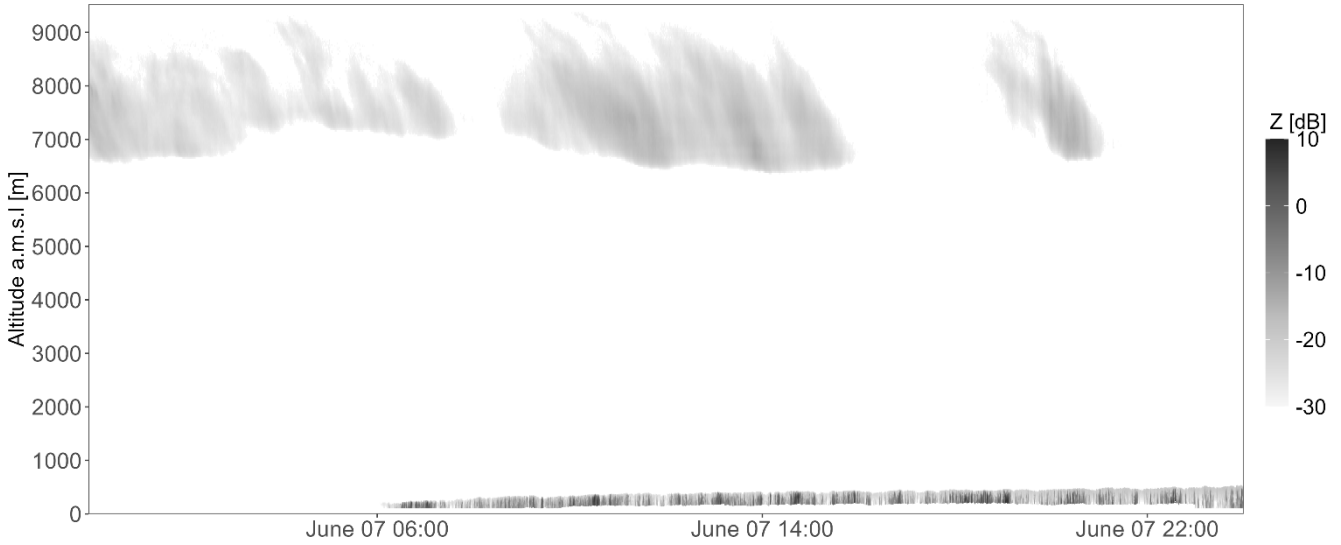

Figure S6 Time series of radar reflectivity, indicating the presence of clouds up to 10'000 m above sea level on June 7, 2023.

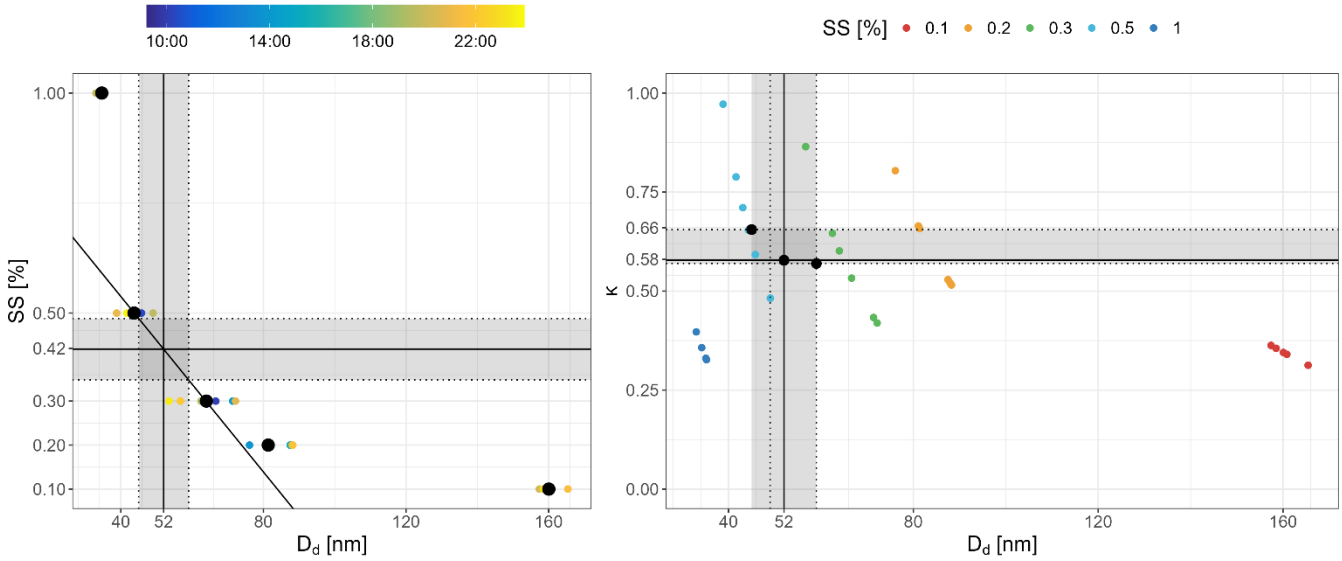

Figure S7 (a) Calculated critical activation diameters (D_d) for different supersaturation levels of the CCNC throughout the day on June 7, 2023. Black dots represent the daily average for each supersaturation. The black line represents a linear interpolation between two supersaturation levels, used to estimate the cloud's supersaturation for a D_d of 52 nm (i.e., measured Hoppel minimum). Grey shadings indicate uncertainty ranges corresponding to 10 % of the Hoppel minimum. (b) Calculated κ-values as a function of D_d and supersaturation. The black dots represent the best estimate and uncertainty range, highlighted by the grey shading.

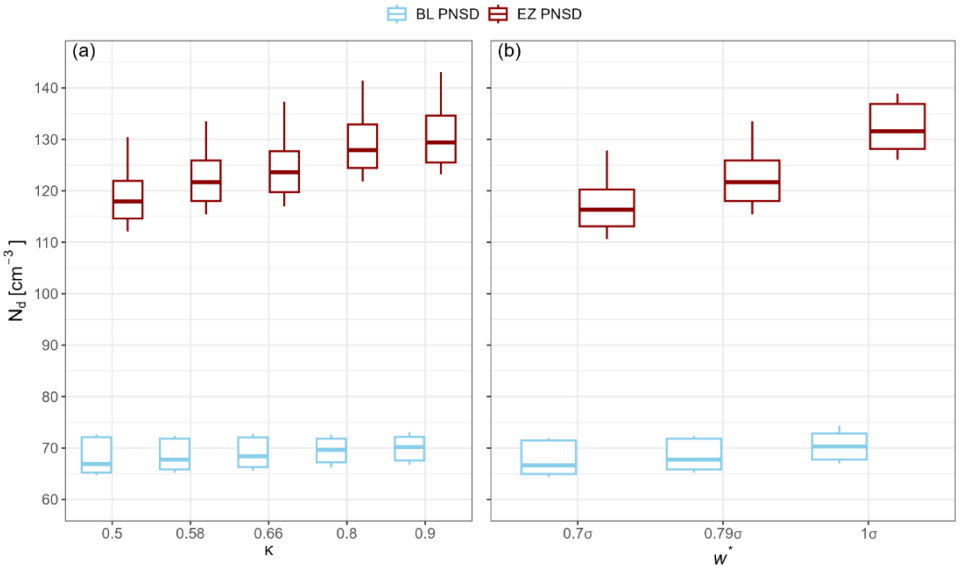

Figure S8 (a) Boxplot of droplet numbers from the aerosol activation parametrization using the boundary layer PNSD (blue) and entrainment zone PNSD (dark red) as inputs for different κ-values. (b) Parametrized maximum supersaturation with the two different PNSD inputs for different characteristic velocities. The boxplots represent the median and interquartile range, the whiskers' length equals to 1.5 times the interquartile range.

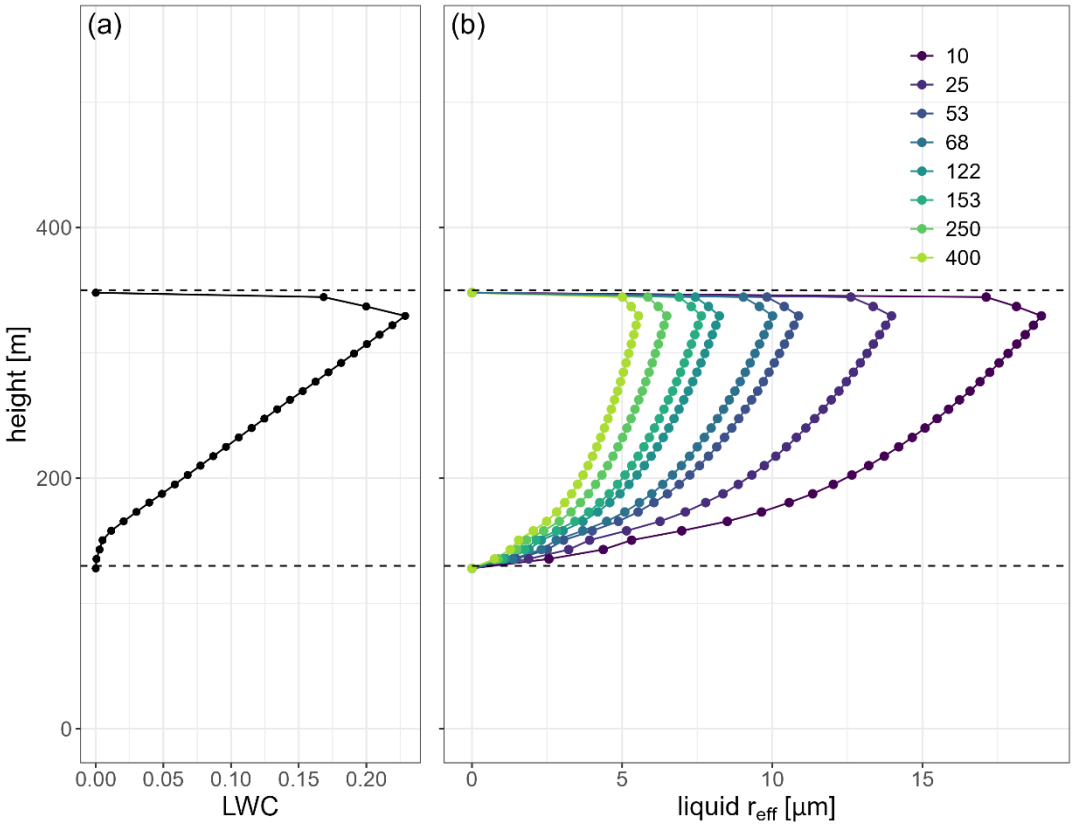

Figure S9 Profiles of (a) average liquid water content between 11:30 and 11:45 obtained from the remote sensing instruments and (b) cloud droplet effective radius (r_{eff}) for different cloud droplet number concentration profiles.